Assessing the Accuracy of Software in Identifying Atherosclerotic Plaque Composition

Name: Esther Staats

Student ID: 6418090

Supervisors: Michiel Poorthuis (resident neurology University Medical Center Utrecht)

Ynte Ruigrok (neurologist University Medical Center Utrecht)

Department: Neurology

Period: 15th of January 2024 - 5th of April 2024

Abbreviations

AUC = area under curve value

BMI = body mass index

CEA = carotid endarterectomy

CTA = computed tomography angiography

HU = Hounsfield units

IPH = intraplaque hemorrhage

IQR = interquartile range

LAA = large artery atherosclerosis

LRNC = lipid rich necrotic core

No. = Number

SD = standard deviation

TIA = transient ischemic attack

UMCU = University Medical Center Utrecht

Abstract

Introduction

Carotid stenosis is a common cause for ischemic stroke and can be diagnosed through computed tomography angiography. Certain plaque characteristics are suggested to increase risk of ipsilateral ischemic stroke. This study aims to evaluate the accuracy of semi-automated software in identification of plaque tissue types by comparison with histology.

Methods

Patients, who had a preoperative computed tomography angiography and underwent carotid endarterectomy were included. Computed tomography angiographies were analyzed with semi-automated software to identify the composition of carotid plaques (dense calcium, fibrous tissue, fibrofatty tissue, and necrotic core). During pathological examination, plaque tissue types were scored (calcifications, collagen, fat, macrophages and intraplaque hemorrhage) and dichotomized. The software-derived and histological values were compared to evaluate the discriminative performance of the software.

Results

After exclusion of 59 patients, 44 were eligible for inclusion. Calcifications and macrophages could be significantly ($p<0.05$) discriminated on computed tomography angiography with an area under curve of 0.88 (95% CI 0.77-0.98) and 0.76 (95% CI 0.61-0.90) respectively. However, the area under curve of the discriminative ability of collagen and fat was 0.69 (95% CI 0.46-0.92) and 0.67 (95% CI 0.51-0.84) respectively, which did not achieve significance ($p>0.05$). The diagnostic accuracy for detecting the presence of intraplaque hemorrhage was low (area under curve = 0.40, 95% CI 0.19-0.60; $p>0.05$).

Conclusion

Semi-automated software has some, but limited accuracy in identification of plaque tissue types compared to histological evaluation. Further research should be conducted to more accurately determine the correspondence of semi-automated software with histology.

Higher quality tables and figures are available in the appendix.

Introduction

Ischemic stroke is one of the leading causes of death in Europe, accounting for approximately 1.4 million new cases every year and contributing to 1.1 million deaths.[1] The rising incidence of ischemic stroke emphasizes the need for comprehensive understanding and effective management.[2] A stroke is characterized by neurological disability, such as numbness, aphasia, ataxia and paralysis, which poses a significant health challenge.[3] The European Society for Vascular Surgery[1] defines a stroke as a sudden onset neurological disability of vascular origin, lasting at least 24 hours. A transient ischemic attack (TIA) shares similar symptoms, but these symptoms remit within 24 hours.[1] The manifestation and localization of clinical symptoms depend on the function of the occluded artery[3].

The Trial of Org 10172 in acute stroke treatment defines five categories of etiology for stroke/TIA, including large-artery atherosclerosis (LAA), cardioembolism, small-artery occlusion (lacune), stroke of other determined etiology and stroke of undetermined etiology.[4] LAA contributes to approximately 15.3% to 27% of all ischemic strokes.[5,6,7] The diagnostic approach to identify LAA with imaging involves computed tomography angiography (CTA) and Magnetic Resonance Angiography, with CTA being the preferred imaging modality in most hospitals.[8] For severe (70-99%) symptomatic stenosis and to lesser extent for moderate symptomatic stenosis (50-69%) carotid endarterectomy (CEA) has been found to reduce the risk of future ischemic cerebral events.[9,10,11] For asymptomatic patients CEA is considered when the carotid stenosis is more than 60% and when stroke risk is increased by at least one clinical or imaging feature (e.g. silent ipsilateral infarction, stenosis progression >20%, intraplaque hemorrhage on MRI, plaque lucency on duplex ultrasonography, etc.).[1] Asymptomatic patients with stenosis exceeding 50% could be offered annual carotid artery follow-up with duplex ultrasonography to monitor plaque progression.[1]

Recently, a shift in knowledge about carotid stenosis has occurred, emphasizing not only the stenosis grade, but also characteristics of the carotid plaque in influencing the risk of future cerebral ischemic events.[12] In the development of an atherosclerotic plaque, low-density lipids infiltrate the endothelium of a vessel, leading to the formation of a fatty streak. As the plaque grows and macrophages infiltrate, a necrotic core is created. The plaque is strengthened by a cover of fibrous tissue, mainly consisting of smooth muscle cells and collagen.[13,14] A systematic review by Baradaran et al.[15] underscores the significance of plaque features on CTA and their association with ipsilateral ischemic strokes. The findings suggest an increased risk in patients with soft plaque, plaque ulceration and increased wall thickness and a reduced risk in patients with calcified plaques. Predictors of high ipsilateral ischemic stroke risk have also been identified for magnetic resonance imaging (MRI), such as intraplaque hemorrhage (IPH),[16,17,18,19] lipid rich necrotic core (LRNC) [18,20], thin fibrous cap[18,20] and total plaque volume[16,21]. On CTA some of these components manifest as a “soft” or “fibrofatty” plaque, which includes IPH, LRNC and fibrous elements.[22]

Plaque characteristics are becoming more important in the decision making for CEA.[1] Studies evaluating the accuracy of CTA characterization of plaques compared with histology have been conducted, but often suffer from small sample sizes or low accuracy with the used software. Standardized protocols are necessary for incorporating these high-risk features into treatment decisions, because they could facilitate to the differentiation between patients requiring a CEA and those who do not.[15] To address this, new semi-automated software (QAngioCT, Medis Medical Imaging, The Netherlands) has been developed to identify plaque composition on CTA. This study will evaluate the diagnostic accuracy of QAngioCT by comparing the software’s

analysis with the histopathological findings of the carotid plaque following CEA.

Methods

Patient selection

Current retrospective study consists of patients included in the Athero-Express database. This involves adults undergoing a CEA in the University medical center Utrecht (UMCU) or St Antonius Hospital Nieuwegein between 2005 and 2018. The Medical Ethics Review Committee approved the study protocol and all of the patients gave informed consent for use of their medical information for research purposes. Information about the database has been previously described in more detail.[23] The database provided patient characteristics and information about the plaque composition. Preoperative CTAs were extracted from electronic health records. Concerning the CTAs, patients without an available preoperative CTA, poor imaging quality (e.g. few images, scattering interfering with the stenosis, ill-timed contrast bolus, motion artifact, etc.) and severe stenosis extending to the cranium were excluded. Regarding the histology, patients without relevant histological data about the plaque characteristics were also excluded.

Data extraction

Information about the patients was already collected in the database. Partly, data were extracted from electronic health records, including gender, symptoms due to the carotid stenosis (asymptomatic, ocular symptoms including amaurosis fugax and retinal artery occlusion, TIA or stroke), side of the operation (left or right), pulse pressure (difference between systolic pressure and diastolic pressure) and body mass index (BMI; calculated with height and weight and based on the world health organization classification). Additional characteristics were gathered by filling in a questionnaire by the patient, including presence of diabetes mellitus, history of heart disease (cardiovascular artery disease, myocardial infarction and/or coronary intervention), history of peripheral artery occlusive disease (femoral intervention, claudication or ankle-brachial index <0.70), use of antihypertensive drugs, use of statins or lipid lowering drugs and current or past smoking habits.

Histology protocol

Details about the histological protocol of the carotid plaques are described previously.[23,24] In short, during CEA the atherosclerotic plaque is dissected from the carotid artery by a surgeon and directly transported to the laboratory. The plaque is divided in parts of 0.5 cm and the culprit lesion is fixated in formaldehyde 4% and paraffin embedded. A pathologist cuts 15 slices of 5 μm thickness to determine the histological parameters. For identification of the tissue types the following stainings were used: Picro Sirius red staining with the use of polarized light to identify fat and collagen, CD68 staining to identify macrophages, hematoxylin and eosin staining to identify calcifications and hematoxylin and eosin with fibrin staining to identify IPH. Two independent observers microscopically scored the sections semi-quantitatively. The presence of collagen, calcifications and macrophages was marked as “no”, “minor”, “moderate” or “heavy” staining. Collagen was marked as “no” or “minor” when no or part of the luminal border was stained; it was marked as “moderate” or “high” in case of staining across the whole luminal border. Calcifications were “no” or “minor” stained when no or only scattered spots were identified; it was scored as “moderate” or “high” when evident areas of calcification were visible. The presence of macrophages was marked as “no” or “minor” staining when they were absent or when only few scattered cells were visible; it was marked as “moderate” or “heavy” staining when clusters of at least 10 cells were present. Macrophages were rated as percentage of the plaque using computerized analyses. The presence of fat was scored as less than 10%, between 10% and 40% more than 40% of the plaque. Intraplaque hemorrhage was defined as a bleeding within the tissue of the plaque and determined as present or absent. In case of disagreement of the interpretation of a section, a third independent observer analyzed the plaque.

CTA imaging protocol

Different preoperative CTAs were used, involving 16-sections scanners, 64-sections scanners and 256-sections scanners (Philips) with slice thickness differing between 0.67 mm and 1.0 mm. All scans were performed using intraluminal contrast to enhance the discriminability of the lumen of the carotid arteries. All CTAs extended from the aortic arch to the cranial vertex.

Imaging analysis

The CTAs were analyzed with semi-automated software (QAngioCT, Medis medical imaging systems). CTAs were extracted from patient records and uploaded into the software system. After a training video from the software developers and sufficient explanation by a former user, a reviewer evaluated the CTAs using the semi-automated software.

Primarily, the common carotid artery and internal carotid artery were identified by the reviewer. The software presented the area of the arteries longitudinally and transversely. Lumen and vessel wall contours were defined by the software and manually adjusted by the reviewer. The proximal boundary, distal boundary and the biggest obstruction site of the stenosis were marked based on visual inspection. In case of multiple lesions, only the lesion near the bifurcation was used for analysis. After applying the contours and lesions, the software analyzed the plaque components. Hounsfield unit differences discriminated between necrotic core, fibrofatty, fibrous and dense calcium tissues with ranges from -30 to 75, 76 to 130, 131 to 350 and higher than 351 respectively. The individual tissue types could be visualized within the CTA images with a color overlay *(Figure 1)*.

Except for the side of the operation, the reviewer was blinded for the patient and plaque characteristics during analysis of the CTAs. In case of doubt about the interpretation of the imaging, the reviewer discussed the CTA with an experienced neurologist or, in specific cases, with an experienced neuroradiologist until agreement was achieved. The first 24 scans were re-evaluated by the reviewer after discussing the interpretation of the scans with the neurologist.

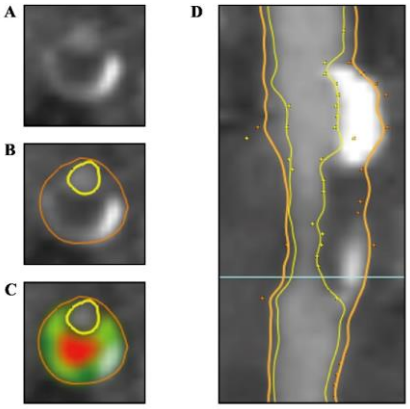

Figure 1. *Example of the QAngioCT software*
Transversal and longitudinal slice visualizing the left carotid artery, containing a narrowed lumen and an atherosclerotic plaque. (A) Transversal slice without formatting. (B) Transversal slice with additional lumen (yellow) and vessel wall (orange) contours. (C) Transversal slice with contours and color overlay defining the tissue types (red = necrotic core, light green = fibrofatty, dark green = fibrous, white = dense calcium). D, Longitudinal slice with lumen (yellow) and vessel wall (orange) contours, with a light blue line indicating the location of the transversal slice (as can be seen in A, B and C).

Statistical analysis

For continuous data, means and standard deviations (SDs) were calculated. Categorical variables were presented as absolute numbers with percentages.

Histological data was dichotomized into two categories to strengthen the effect of the results in a relatively small cohort. The presence of collagen, calcifications and macrophages were classified as “low” in case of no or minimal staining and as “high” in case of moderate or heavy staining. Fat was categorized as “low” or “high” with the cut-off value of 40% of the plaque. IPH was categorized as “present” or “absent”. The proportions of the different software characteristics were calculated by dividing tissue volume by the total plaque volume. Continuous proportions were compared with the dichotomous histological data (dense calcium with calcifications, fibrous tissue with collagen, fibrofatty tissue with fat and necrotic core with macrophages and IPH respectively). Normality of the software-based data was determined using the Shapiro-Wilk test. In case of a normal distribution, the significance of the difference between the software-derived data from two histological subcategories ("low" and "high" or "present" and "absent") was calculated with the Independent Samples t-Test and mean values with SDs were determined. In case of non-normally distributed data, the significance of the difference of the software-derived data

between two histological subgroups was calculated with the Mann-Whitney U test and the median values with interquartile ranges (IQRs) of the software data were determined. Scatterplots with mean value or median value and p-values were generated using Excel (Microsoft 365) to visualize the correspondence between software values and histological values. Receiver operator characteristic curves were created and area under curve (AUC) was calculated to evaluate the accuracy of the continuous software data with the binary histological data as reference standard. Statistical analyses were computed using IBM SPSS Statistics 29 and statistical significance of the difference of the software data between the two subgroups of the histological parameter was achieved when $p < 0.05$.

Results

The Athero-Express database consists of 2758 patients who underwent CEA, with 1707 surgeries performed at the UMCU. Among these, 461 CTAs from the UMCU were available for software analysis. Due to time constraints, only 103 patients were initially considered for inclusion in the study, of which 44 patients were found eligible (*Figure 2*). Based on CTA, 40 patients were excluded: 31 patients due to scattering interfering with the plaque, mainly because of dental prostheses; 2 patients due ill-timed contrast bolus; 5 patients due to poor quality of the CTA; 1 patient due to severe stenosis extending to the cranium; and 1 patient due to motion artifacts. After CTA analysis another 19 patients were excluded due to lack of histological data.

As is outlined in *Table 1*, the mean age of the included patients was 69.4 (SD: 9.5) years, 34 (77.3%) were male, 33 (76.7%) had a symptomatic stenosis and 29 (65.9%) had the operation left-sided. Concerning the cardiovascular risk factors, 16 (36.4%) patients had diabetes mellitus, 18 (40.9%) and 12 (27.3%) patients had a history of heart or peripheral artery occlusive disease respectively. Antihypertensive drugs were used by 31 (70.5%) patients with a mean pulse pressure of 66.5 mmHg (SD = 17.6) and 37 (84.1%) patients used statins or other lipid lowering drugs. For 25 (59.5%) patients the BMI was higher than normal (>25 kg/m²) and 34 (77.3%) patients smoked or had smoked.

A summary of the histological and software-based data is available in *Table 2*. According to

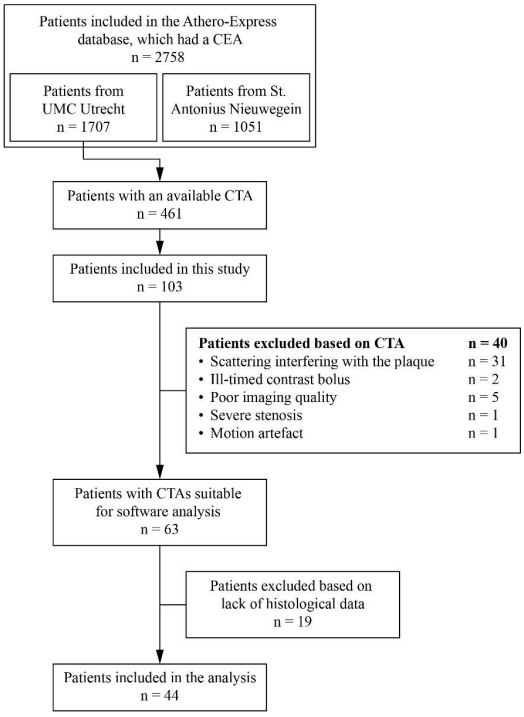

Figure 2. *Inclusion of patients based on the selection criteria*
CEA = coronary endarterectomy; UMC = University medical center; CTA = coronary tomography angiography

Table 1.
Characteristics of all included patients.

Variable	No. of patients (%) (average ± SD for age and pulse pressure) (n = 44)*	Missing values
Age (year)	69.4 ± 9.5	
Male sex	34 (77.3)	
Symptomatic	33 (76.7)	1
Ocular†	5 (11.6)	
TIA	15 (34.9)	
Stroke	13 (30.2)	
Operation on left side	29 (65.9)	
Cardiovascular risk factors		
Diabetes mellitus	16 (36.4)	
History of heart disease**	18 (40.9)	
History of peripheral artery occlusive disease***	12 (27.3)	
Pulse pressure (mmHg)	66.5 ± 17.6	
Use of antihypertensive drug	31 (70.5)	
Use of statin or lipid lowering drug	37 (84.1)	
BMI††		2
Underweight	1 (2.4)	
Normal	16 (38.1)	
Overweight	17 (40.5)	
Obese	8 (19.0)	
Smoker†††	34 (77.3)	

No. = number; SD = standard deviation; TIA = transient ischemic attack; BMI = body mass index.
Data about the patient characteristics was not available for all patients.
* n = 44, unless there are missing values.
** History of heart disease includes cardiovascular artery disease, myocardial infarction and/or coronary intervention
*** History of peripheral artery occlusive disease includes femoral intervention, claudication or ankle-brachial index <0.70.
† Ocular symptoms include amaurosis fugax and retinal artery occlusion
†† BMI categorized based on world health organization classification, defining underweight as <18.5 kg/m²; normal weight as 18.5 kg/m² to 25 Kg/m²; overweight as 25 kg/m² to 30 kg/m²; and obese as >30 kg/m².
††† Smoker is defined as current or former smoker

the software-based data, the average proportion of different tissue types for all patients was quite similar, ranging from 22.7% to 29.5% of the whole plaque. The proportion of dense calcium and necrotic core differed over a broader range (0.0% to 80.6% and 0.7% to 75.4% respectively) compared to fibrous and fibrofatty tissue (12.6% to 49.3% and 1.4% to 51.4% respectively). Histology-based data of the tissue types were not fully available for all patients. The presence of collagen, macrophages and IPH was only available for 31, 41 and 42 patients respectively. According to histology, a high presence of collagen, macrophages and IPH was present in most plaques (71.0%, 51.2% and 69.0% respectively) and this number was lower for calcifications and macrophages (29.5% and 27.3% respectively).

The comparison between the software-based data and the histological data with mean or median values is visualized in scatterplots (*Figure 3*). The distribution of the software-based proportions of dense calcium appear to differ significantly between the "low" (median = 6.25%, IQR 2.5%-24.1%) and "high" (median = 49.69%, IQR 27.8%-55.1%) category of the histological calcifications ($p<0.001$). In addition, the software-based necrotic core also significantly ($p=0.005$) differs between the histological categories of macrophages with medians of 9.7% (IQR 2.9%-29.1%) and 28.05% (IQR 15.3%-51.3%) respectively. However, the other comparisons of the software-based data between the two histological subgroups do not show a significant difference with mean values of 26.4% (SD=7.4; for low presence) and 30.8% (SD=8.7; for high presence) for software-based fibrous tissue compared to histology-based collagen ($p=0.193$); mean values of 21.3% (SD=11.0; for low presence) and 26.5% (SD=7.5; for high presence) for software-based fibrofatty tissue compared to histology-based fat ($p=0.141$) and median values of 24.98% (IQR 6.9%-56.7%; for absence) and 22.07% (IQR 6.3%-32.3%; for presence) for software-based necrotic core compared to histology-based IPH ($p=0.305$).

Regarding the diagnostic accuracy, the high presence of calcium was identifiable by dense calcium from the software with an AUC of 0.88 (95% CI 0.77-0.98). Although to a lesser extent, the high presence of macrophages identified in histology could be discriminated by the software-based necrotic core with an AUC of 0.76 (95% CI 0.61-0.90). The discriminative performance of the histologically found collagen and fat, identified by the software-based fibrous and fibrofatty tissue, respectively, was acceptable (AUC values of 0.69, 95% CI 0.46-0.92 and 0.67, 95% CI 0.51-0.84 respectively). Furthermore, the presence of IPH cannot be identified with the software parameter necrotic core to any extent (AUC = 0.40, 95% CI 0.19-0.60). These results are also presented in *Table 3*.

Table 2.
Prevalence of individual tissue types as noted by the software and histology

	Software-based data†		
Variable	**No. of plaques**	**Mean proportion, in % ± SD (range)**	
Dense calcium	44	23.0 ± 21.6 (0.0 - 80.6)	
Fibrous	31	29.5 ± 8.4 (12.6 - 49.3)	
Fibro-fatty	44	22.7 ± 10.4 (1.4 - 51.4)	
Necrotic core	42	24.6 ± 20.4 (0.7 - 75.4)	
	Histology-based data††		
		No. of plaques with low/high presence in n (%)	
		Low/absent*	**High/present***
Calcifications	44	31 (70.5)	13 (29.5)
Collagen	31	9 (29.0)	22 (71.0)
Fat	44	32 (72.7)	12 (27.3)
Macrophages	41	20 (48.8)	21 (51.2)
IPH	42	13 (31.0)	29 (69.0)

No. = number; SD = standard deviation; IPH = intraplaque hemorrhage
Data about the histology of the plaque was not available for all patients. For the software-based data only the number of plaques are included of the available corresponding histological tissue type.
* The histology-based data was categorized in "low" and "high" presence, except for IPH, which was categorized in "absent" and "present".
† The software-based data represents the percentage of a specific tissue type compared to the whole plaque according to semi-automated software, which was used to analyze the CTA.
†† The histology-based data was measured by pathological examination and scored in subgroups of presence (low or high and in case of IPH absent or present).

Table 3.
The discriminative performance of the software by comparing the software-based proportions with the histology-based high presence of the tissue types.

Software parameter†	Histology parameter††	AUC (CI 95%)
Dense calcium	Calcifications	0.88 (0.77 - 0.98)
Fibrous	Collagen	0.69 (0.46 - 0.92)
Fibro-fatty	Fat	0.67 (0.51 - 0.84)
Necrotic core	Macrophages	0.76 (0.61 - 0.90)
Necrotic core	IPH	0.40 (0.19 - 0.60)

AUC = area under curve value; CI = confidence interval; IPH = intraplaque hemorrhage
† The software parameter defines an individual tissue type based on software used to analyze the CTA (dependent on HU values of the tissue type on CTA), measured in percentages of the whole plaque.
†† The histology parameter defines an individual tissue type based on histological examination of the culprit slice of the plaque, scored as low or high presence and in case of IPH present or absent.

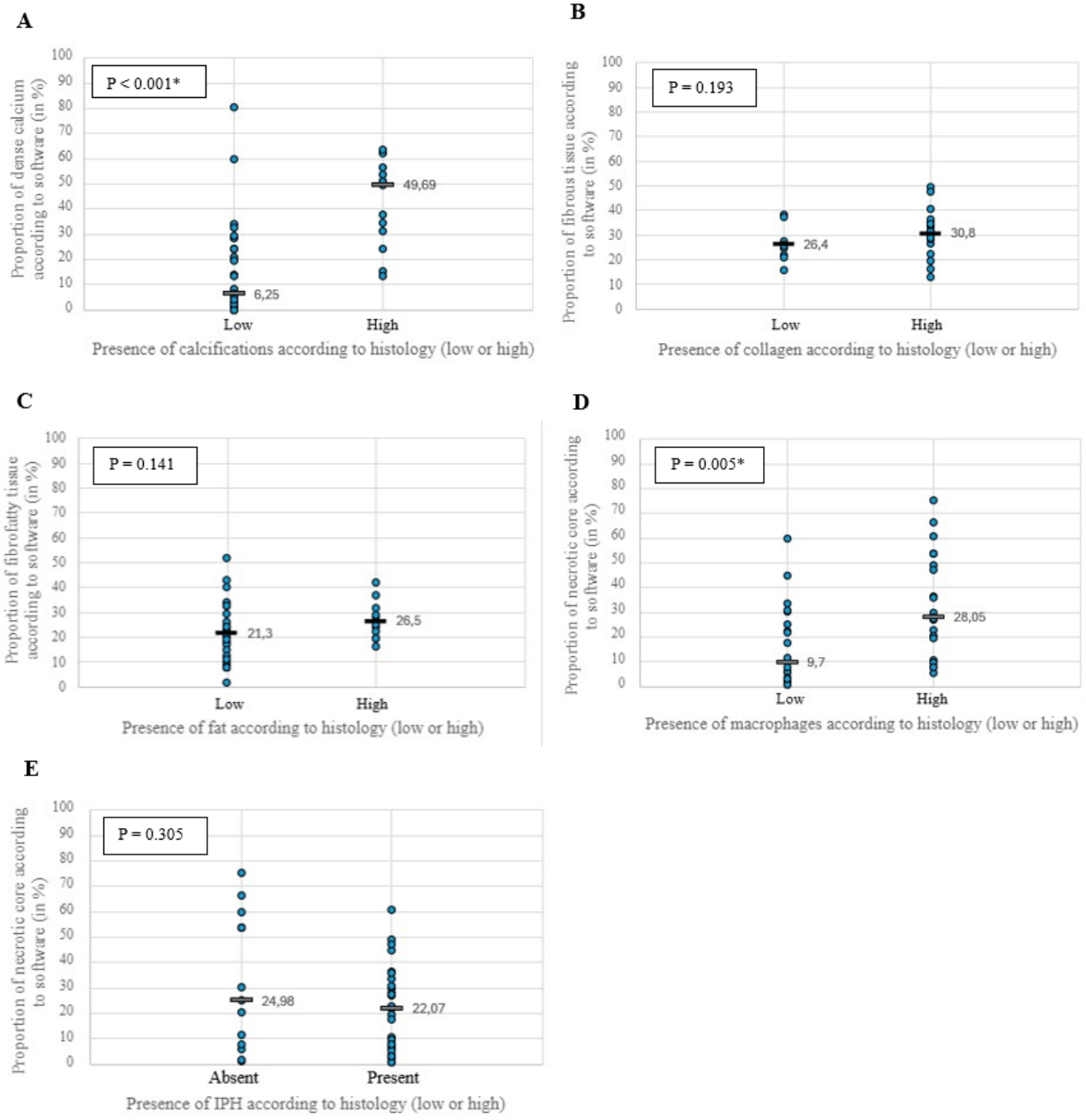

Figure 3.

Scatterplots of the distribution of the software-derived data, divided by the histological subcategories (low/absent or high/present). The p-values indicate the significance of the difference of the software-derived data between the subcategories of the histological data. For normal distribution of the continuous data (in case of B and C), the mean values are presented with black lines and the corresponding value; and the p-value was calculated with Independent Samples t-Test. For non-normal distributions of the continuous data (in case of A, D and E), the median values are presented with grey lines and the corresponding value; and the p-value was calculated with the Mann-Whitney U test. (A) Software-based dense calcium (in %) compared to the histology-based presence of calcifications (low or high). (B) Software-based fibrous tissue (in %) compared to the histology-based presence of collagen (low or high). (C) Software-based fibrofatty tissue (in %) compared to the histology-based presence of calcifications (low or high). (D) Software-based necrotic core (in %) compared to the presence of histology-based macrophages (low or high). (E) Software-based necrotic core (in %) compared to the histology-based presence of IPH (absent or present).

IPH = intraplaque hemorrhage

* $P < 0.05$ is significant

Discussion

The aim of this study was to evaluate the accuracy of semi-automated software (QAngioCT, Medis medical imaging systems) in characterizing tissue types in an atherosclerotic plaque at the site of the carotid artery with histology as reference standard. The results indicated that the semi-automated software is able to identify a high proportion of calcifications and macrophages reliably. Although a high proportion of collagen and fat seemed to be discriminable, this study did not show significance. In addition, IPH could not be discriminated by the software to any extent.

Existing literature

The characterization of plaque tissues has been studied before, using different methods and attenuation thresholds (*Table 4*). Some articles determined attenuation thresholds based on regions of interest, which were used to compare tissue areas from CTA with histology in the same study sample.[25,26] Varrassi et al.[27] used predefined cut-off values and software, similar to this study. The cut-off values of the individual articles differed from 39.5 to 60 HU between lipid and fibrous/connective tissue, whereas the threshold for calcification ranged from ≥130 to ≥177.1 HU and higher. Wintermark et al.[26] also differentiated hemorrhage with a range of 72 to 177.1 HU. Saba et al.[28] studied the average attenuation for IPH, LRNC and fibrous tissue and found 17.5 HU (SD 4.9), 39.5 HU (SD 19.5) and 91.7 HU (SD 17.7) respectively. These thresholds differ from those used in this study, in which the cut-off values of necrotic core (compared with macrophages and IPH), fibro-fatty tissue (compared with fat), fibrous tissue (compared with collagen) and dense calcium (compared with calcifications) were determined at -30 to 75, 76 to 130, 131 to 350 and >350 HU respectively. These values are based on intravascular ultrasound virtual histology at the site of a coronary plaque[29] and were optimized in training sets.[30] For future research the cut-off values of the tissue types on the CTA need to be assessed more thoroughly.

Calcifications are known to create a so-called "blooming effect", causing an overestimation of the calcium volume and consequently the overestimation of the stenosis severity. It, thereby, hinders the accurate identification of adjacent tissue.[31] Sheahan et al.[32] and Benson et al.[33] used the software VascuCAP (Elucid Bioimaging Inc., Wenham), which not only relies on HU thresholds, but also on attenuation distributions within the imaging to minimize interference of the blooming effect.[34] The semi-automatic software in this study does not take this interference into account. Consequently, this could have affected the observed outcomes by overestimating calcifications and underestimating of other tissue types.

Li et al.[35] identified plaque composition using a dual-layer spectral detector CTA, which enhances the visualization and characterization of arteries compared with conventional CTA. They determined the average attenuation values of the individual tissue types for conventional as well as monoenergetic CTAs. By comparing imaging with histological regions of interest, discrimination between the tissue types could be examined. Regions with more than one histological component were excluded from the analysis.

In context of the literature

Table 4.
Attenuation thresholds/values for each tissue type according to current and previous studies.

Article	Attenuation thresholds for each tissue type (in HU) (and mean attenuation per tissue type for Saba et al.)
De Weert et al.*	Lipid core: -20 to 60 Fibrous: 60 to 140 Calcifications: >130
Wintermark et al.*	LRNC: < 39.5 Connective tissue: 39.5 to 72 Hemorrhage: 72 to 177.1 Calcification: >177.1
Varrassi et al.**	Adipose: -100 to 49 Fibrotic: 50 to 150 Calcifications: >150
Saba et al.***	IPH: 18.4 ± 4.8 LRNC: 48.048 ± 19.4 Fibrous: 93.128 ± 16.4
Current study†	Necrotic core: -30 to 75 Fibrofatty: 76 to 130 Fibrous: 131 to 350 Dense calcium: >350

HU = Hounsfield unit; SD = standard deviation; LRNC = lipid rich necrotic core; IPH = intraplaque hemorrhage
* Attenuation thresholds/values based on histological tissue regions compared with HU values on CTA.
** Reasoning for attenuation thresholds unclear.
*** Mean attenuation values were described instead of attenuation thresholds. These values were based on histological tissue regions compared with HU values on CTA.
† Attenuation thresholds based on intravascular ultrasound virtual histology of coronary artery and optimized training sets.

Regarding calcifications, our results are similar to other articles.[25,26,27,32,33] Benson et al.[33] measured the AUC of different tissue types in the atherosclerotic plaque from the carotids and found for calcifications an AUC of 0.73, which is lower than our study result with an AUC of 0.88 (95% CI 0.77-0.98). Despite the use of another software system, this difference may also be explained by the fact Benson et al. subcategorized the absence of calcification, while this study combined both the absence of calcification and minor calcifications into the category "low".

As to our knowledge, this study is the first to look into the discriminative ability of macrophages on CTA. A lipid rich region can turn into a necrotic core by the invasion of macrophages, which create a combination of lipids and cell debris.[14] Surrounding cells go into apoptosis and are removed inadequately, which enhances oxidative stress and deprivation of nutrients. This contributes to more cell death and leads to an accumulation of necrotic tissue.[13] According to our study results, the high presence of macrophages can reliably be identified with necrotic core findings on CTA (AUC = 0.76 with 95% CI 0.61-0.90; p=0.005).

Although there seems to be a discriminative ability for the characterization of a high presence of collagen on CTA (AUC = 0.69, 95% CI 0.46-0.92), this is not found to be significant (p = 0.193). Other articles did find a significant discriminative performance for fibrous tissue (extracellular matrix of connective tissue, smooth muscle cells, fibroblasts and inflammatory cells)[25,27], fibrous cap thickness (distance to the surface of non-connective tissue (lipid, blood or calcium))[26] and matrix (collagen, elastin, glycoproteins and proteoglycans)[32]. Apart from the variance in histological reference tissues, another factor that might influence the results could be the relatively small sample size in this study. The significance may increase in case of more included plaques.

Even so, a high presence of fat could not be identified reliably within this study (AUC = 0.67, 95% CI 0.51-0.84; p = 0.141). Varrassi et al.[27] found a significant, but low correlation with adipose tissue. Other studies compared a lipid rich necrotic core and found insignificant[26] or low[25,32,33] associations. However, Wintermark et al.[26] did find a significant discriminative performance with only large lipid cores (massive extracellular lipid pools). The average attenuation value of LRNC also seemed to differentiate significantly compared to other tissues according to research.[28,35]

In this study, IPH could not be identified with the software, which is similar to Wintermark et al.[26] Other studies suggest a significant, but diagnostically low performance.[33,35] The identification of IPH with CTA is difficult, because of overlapping HU values with other tissue types.[26,28,34] In addition, Wintermark et al.[26] determined a HU value higher than fibrous tissue and lipid core, while Saba et al.[28] suggested the opposite and Li et al.[35] found the HU value of IPH only higher than LRNC, but lower than fibrous tissue. A reason for this variation could be the different stages of IPH, including recent, organized, amorphous and amorphous with calcifications.[36] Differentiating between these phases could increase the correlation with imaging.

Clinical implications

A literature review of Saba et al.[21] suggests a higher stroke risk in patients with plaques containing IPH, LRNC, macrophages and a thin fibrous cap. A heavily calcified plaque is associated with a lower stroke risk. Characterization of plaque composition plays a vital role in identifying patients with high stroke risk. This characterization could be used in the decision making concerning surgery, especially for asymptomatic patients.

Strengths of this study

One of the strengths of this study involves the use of the large and ongoing Athero-Express database, which creates the possibility to include a large group of patients to contribute to the accuracy of the results. The database already consists of almost three thousand patients, who underwent CEA.

Another strength is that the current study involves higher slice CTAs compared to

previous articles,[25,26,28,33] leading to better image quality. Increased precision of the imaging is presumably beneficial for the characterization of plaque components.

The third strength involves the examination of the discriminative performance of macrophages on CTA. There has not been another article pointing out this ability, whilst it seems to be an important histological marker for vulnerable plaques.

Limitations

This study also has some limitations. Concerning the available histological data, only the culprit 0.5cm was evaluated during histological evaluation, whereas the software analysis included the whole plaque. As a result, the assumption had to be made that the characteristics of the culprit slice reflect the composition of the whole plaque. Other articles matched a specific histological region with the corresponding region on CTA, enhancing the comparability between the outcomes.[25,26,32] Besides, due to the retrospective design of the study, most of the gathered pathological data could not directly be related to a specific software parameter. Therefore, discrepancies between the data and software parameters exist, thus limiting the comparability. In addition, the histological parameters were only examined categorically and dichotomized due to a limited amount of included patients. Instead, describing the amount of pathological tissue types continuously using percentages, rather than categorically, could lead to more precise results.

Furthermore, regarding the CTA analysis, the reviewer was not familiar with evaluating CTAs beforehand. In previous studies the CTAs were analyzed by an experienced (neuro)radiologist.[26,27,28,32,33] This may have influenced the accuracy of the CTA evaluation, reducing the true value of the software. In addition, in other articles the evaluation of CTAs between two independent reviewers seemed to show some variability.[25,32] This underlines the importance to adhere to unambiguous evaluation methods to optimize the reproducibility of the results.

Future research

This study demonstrates some discriminative ability of CTA compared to the true histological components of an atherosclerotic plaque in the carotid arteries by using semi-automated software. The next step in the process would be to observe the effects of using CTA characterization in the decision making for CEA. However further research is needed to validate the discriminative performance found in this study, especially regarding cut-off values and the discrepancies in the comparison between the software parameters and histological data. Future studies should also focus on more developed imaging techniques like spectral CTAs, which seem to differentiate more clearly between non-calcified tissue types.[35] It would also be interesting to evaluate the different stages of IPH, because of their potentially unique appearances on CTA. More elaborate research on this topic may improve the discriminative performance of CTA compared to histology.

Conclusion

The identification of plaque tissue types in a carotid artery on CTA with the use of semi-automated software (QAngioCT, Medis medical imaging systems) partially correspond with histopathological examination. The software shows significant ability in characterizing high presence of calcifications, and macrophages compared to histology. However, while the values of the software seem to be discriminable for histologically identified fat, as well as collagen, these do not appear to be reliable. Furthermore, the software-based values cannot be correlated with IPH found in histology. These outcomes highlight the need for further research to determine more accurately the extent of the correspondence between software and histological tissue types. Improved understanding could assist in the utility of CTA-based plaque characterization in managing carotid artery disease.

References

1. Naylor R, Rantner B, Ancetti S, de Borst GJ, De Carlo M, Halliday A, et al. European Society for Vascular Surgery (ESVS) 2023 Clinical Practice Guidelines on the Management of Atherosclerotic Carotid and Vertebral Artery Disease. Eur J Vasc Endovasc Surg. 2023 Jan 1;65(1):7–111.
2. Wafa HA, Wolfe CDA, Emmett E, Roth GA, Johnson CO, Wang Y. Burden of Stroke in Europe: Thirty-Year Projections of Incidence, Prevalence, Deaths, and Disability-Adjusted Life Years. Stroke. 2020 Aug 1;51(8):2418–27.
3. Murphy SJ, Werring DJ. Stroke: causes and clinical features. Med (United Kingdom). 2020 Sep 1;48(9):561–6.
4. Adams HP, Bendixen BH, Kappelle ; L Jaap, Biller J, Love BB, David ;, et al. Classification of Subtype of Acute Ischemic Stroke Definitions for Use in a Multicenter Clinical Trial. Stroke. 1993 Jan;24:35-41.
5. Kolominsky-Rabas PL, Weber M, Gefeller O, Neundoerfer B, Heuschmann PU. Epidemiology of Ischemic Stroke Subtypes According to TOAST Criteria. Stroke. 2001 Dec 1;32(12):2735–40.
6. Petty GW, Brown RD, Whisnant JP, Sicks JRD, O'Fallon WM, Wiebers DO. Ischemic stroke subtypes: a population-based study of incidence and risk factors. Stroke. 1999;30(12):2513–6.
7. Flaherty ML, Kissela B, Khoury JC, Alwell K, Moomaw CJ, Woo D, et al. Carotid artery stenosis as a cause of stroke. Neuroepidemiology. 2012 Dec;40(1):36–41.
8. Zerna C, Thomalla G, Campbell BC V, Rha J-H. Current practice and future directions in the diagnosis and acute treatment of ischaemic stroke. Lancet. 2018 Oct 8; 392: 1247–56.
9. North American Symptomatic Carotid Endarterectomy Trial Collaborators. Beneficial effect of carotid endarterectomy in symptomatic patients with high-grade carotid stenosis. N Engl J Med. 1991 Aug 15;325(7):445–53.
10. Rothwell PM, Eliasziw M, Gutnikov SA, Fox AJ, Taylor DW, Mayberg MR, et al. Analysis of pooled data from the randomised controlled trials of endarterectomy for symptomatic carotid stenosis. Lancet. 2003 Jan 11;361(9352):107–16.
11. Aboyans V, Ricco JB, Bartelink MLEL, Björck M, Brodmann M, Cohnert T, et al. 2017 ESC Guidelines on the Diagnosis and Treatment of Peripheral Arterial Diseases, in collaboration with the European Society for Vascular Surgery (ESVS). Eur Heart J. 2018 Mar 1;39(9):763–816.
12. Kamtchum-Tatuene J, Noubiap JJ, Wilman AH, Saqqur M, Shuaib A, Jickling GC. Prevalence of High-risk Plaques and Risk of Stroke in Patients With Asymptomatic Carotid Stenosis: A Meta-analysis. JAMA Neurol. 2020 Dec 1;77(12):1.
13. Jebari-Benslaiman S, Galicia-García U, Larrea-Sebal A, Olaetxea JR, Alloza I, Vandenbroeck K, et al. Pathophysiology of Atherosclerosis. Vol. 23, International Journal of Molecular Sciences. MDPI; 2022.
14. Bentzon JF, Otsuka F, Virmani R, Falk E. Mechanisms of plaque formation and rupture. Circ Res. 2014 Jun 19;114(12):1852–66.
15. Baradaran H, Al-Dasuqi K, Knight-Greenfield A, Giambrone A, Delgado D, Ebani EJ, et al. Association between carotid plaque features on CTA and cerebrovascular ischemia: A systematic review and meta-Analysis. Vol. 38, American Journal of Neuroradiology. American Society of Neuroradiology; 2017. p. 2321–6.
16. van Dam-Nolen DHK, Truijman MTB, van der Kolk AG, Liem MI, Schreuder FHBM,

Boersma E, et al. Carotid Plaque Characteristics Predict Recurrent Ischemic Stroke and TIA: The PARISK (Plaque At RISK) Study. JACC Cardiovasc Imaging. 2022 Oct 1;15(10):1715–26.

17. Scott McNally J, McLaughlin MS, Hinckley PJ, Treiman SM, Stoddard GJ, Parker DL, et al. Intraluminal thrombus, intraplaque hemorrhage, plaque thickness, and current smoking optimally predict carotid stroke. Stroke. 2015 Jan 3;46(1):84–90.

18. Gupta A. Carotid Plaque MRI and Stroke Risk. A systematic Review and Meta-analysis. Stroke. 2013 Nov;44(11):3071-7. In.

19. Selwaness M, Bos D, Van Den Bouwhuijsen Q, Portegies MLP, Ikram MA, Hofman A, et al. Carotid Atherosclerotic Plaque Characteristics on Magnetic Resonance Imaging Relate with History of Stroke and Coronary Heart Disease. Stroke. 2016 Jun 1;47(6):1542–7.

20. Kwee RM. Systematic review on the association between calcification in carotid plaques and clinical ischemic symptoms. Vol. 51, Journal of Vascular Surgery. 2010. p. 1015–25.

21. Saba L, Saam T, Jäger HR, Yuan C, Hatsukami TS, Saloner D, et al. Imaging biomarkers of vulnerable carotid plaques for stroke risk prediction and their potential clinical implications. Vol. 18, The Lancet Neurology. Lancet Publishing Group; 2019. p. 559–72.

22. Baradaran H, Gupta A. Carotid vessel wall imaging on CTA. Vol. 41, American Journal of Neuroradiology. American Society of Neuroradiology; 2020. p. 380–6.

23. Verhoeven BAN, Velema E, Schoneveld AH, Paul J, De Vries PM, De Bruin P, et al. Athero-express: Differential atherosclerotic plaque expression of mRNA and protein in relation to cardiovascular events and patient characteristics. Rationale and design. European Journal of Epidemiology 19: 1127–1133, 2004.

24. Hellings WE, Peeters W, Moll FL, Piers S, Van Setten J, Van Der Spek PJ, et al. Composition of carotid atherosclerotic plaque is associated with cardiovascular outcome: A prognostic study. Circulation. 2010 May;121(17):1941–50.

25. De Weert TT, Ouhlous M, Meijering E, Zondervan PE, Hendriks JM, Van Sambeek MRHM, et al. In vivo characterization and quantification of atherosclerotic carotid plaque components with multidetector computed tomography and histopathological correlation. Arterioscler Thromb Vasc Biol. 2006 Oct;26(10):2366–72.

26. Wintermark M, Jawadi SS, Rapp JH, Tihan T, Tong E, Glidden D V., et al. High-resolution CT imaging of carotid artery atherosclerotic plaques. In: American Journal of Neuroradiology. 2008. p. 875–82.

27. Varrassi M, Sferra R, Gravina GL, Pompili S, Fidanza RC, Ventura M, et al. Carotid artery plaque characterization with a wide-detector computed tomography using a dedicated post-processing 3D analysis: comparison with histology. Radiol Medica. 2019 Sep 1;124(9):795–803.

28. Saba L, Francone M, Bassareo PP, Lai L, Sanfilippo R, Montisci R, et al. CT attenuation analysis of carotid intraplaque hemorrhage. Am J Neuroradiol. 2018 Jan 1;39(1):131–7.

29. Brodoefel H, Reimann A, Heuschmid M, Tsiflikas I, Kopp AF, Schroeder S, et al. Characterization of coronary atherosclerosis by dual-source computed tomography and HU-based color mapping: A pilot study. Eur Radiol. 2008;18(11):2466–74.

30. De Graaf MA, Broersen A, Kitslaar PH, Roos CJ, Dijkstra J, Lelieveldt BPF, et al. Automatic quantification and characterization of coronary atherosclerosis with computed tomography coronary angiography: Cross-correlation with intravascular ultrasound virtual histology. Int J Cardiovasc Imaging. 2013 Jun;29(5):1177–90.

31. Pack JD, Xu M, Wang G, Baskaran L, Min J, De Man B. Cardiac CT blooming artifacts: clinical significance, root causes and potential solutions. Vol. 5, Vis Comput Ind Biomed Art. Springer; 2022. p. 29.

32. Sheahan M, Ma X, Paik D, Obuchowski NA, St Pierre S, Newman WP, et al. Atherosclerotic plaque tissue: Noninvasive quantitative assessment of characteristics with software-aided measurements from conventional CT angiography. Radiology. 2018 Feb 1;286(2):622–31.

33. Benson JC, Nardi V, Bois MC, Saba L, Brinjikji W, Savastano L, et al. Correlation between computed tomography angiography and histology of carotid artery atherosclerosis: Can semi-automated imaging software predict a plaque's composition? Interv Neuroradiol. 2022 Jun 1;28(3):332.

34. Varga-Szemes A, Maurovich-Horvat P, Schoepf UJ, Zsarnoczay E, Pelberg R, Stone GW, et al. Computed Tomography Assessment of Coronary Atherosclerosis: From Threshold-Based Evaluation to Histologically Validated Plaque Quantification. J Thorac Imaging. 2023 Jul 1;38(4):226–34.

35. Li Z, Cao J, Bai X, Gao P, Zhang D, Lu X, et al. Utility of Dual-Layer Spectral Detector CTA to Characterize Carotid Atherosclerotic Plaque Components: An Imaging-Histopathology Comparison in Patients Undergoing Endarterectomy. Am J Roentgenol. 2022 Mar 1;218(3):517–25.

36. Mura M, Della Schiava N, Long A, Chirico EN, Pialoux V, Millon A. Carotid intraplaque haemorrhage: pathogenesis, histological classification, imaging methods and clinical value. Ann Transl Med. 2020 Oct;8(19):1273–1273.

Appendix: higher quality tables and figures

Table 1.
Characteristics of all included patients.

Variable	No. of patients (%) (average ± SD for age and pulse pressure) (n = 44)*	Missing values
Age (year)	69.4 ± 9.5	
Male sex	34 (77.3)	
Symptomatic	33 (76.7)	1
Ocular†	5 (11.6)	
TIA	15 (34.9)	
Stroke	13 (30.2)	
Operation on left side	29 (65.9)	
Cardiovascular risk factors		
Diabetes mellitus	16 (36.4)	
History of heart disease**	18 (40.9)	
History of peripheral artery occlusive disease***	12 (27.3)	
Pulse pressure (mmHg)	66.5 ± 17.6	
Use of antihypertensive drug	31 (70.5)	
Use of statin or lipid lowering drug	37 (84.1)	
BMI††		2
Underweight	1 (2.4)	
Normal	16 (38.1)	
Overweight	17 (40.5)	
Obese	8 (19.0)	
Smoker†††	34 (77.3)	

No. = number; SD = standard deviation; TIA = transient ischemic attack; BMI = body mass index.
Data about the patient characteristics was not available for all patients.
* n = 44, unless there are missing values.
** History of heart disease includes cardiovascular artery disease, myocardial infarction and/or coronary intervention
*** History of peripheral artery occlusive disease includes femoral intervention, claudication or ankle-brachial index <0.70.
† Ocular symptoms include amaurosis fugax and retinal artery occlusion
†† BMI categorized based on world health organization classification, defining underweight as <18.5 kg/m^2; normal weight as 18.5 kg/m^2 to 25 Kg/m^2; overweight as 25 kg/m^2 to 30 kg/m^2; and obese as >30 kg/m^2.
††† Smoker is defined as current or former smoker

Table 2.
Prevalence of individual tissue types as noted by the software and histology

	Software-based data†	
Variable	**No. of plaques**	**Mean proportion, in % ± SD (range)**
Dense calcium	44	23.0 ± 21.6 (0.0 - 80.6)
Fibrous	31	29.5 ± 8.4 (12.6 - 49.3)
Fibro-fatty	44	22.7 ± 10.4 (1.4 - 51.4)
Necrotic core	42	24.6 ± 20.4 (0.7 - 75.4)

	Histology-based data††		
		No. of plaques with low/high presence in n (%)	
		Low/absent*	**High/present***
Calcifications	44	31 (70.5)	13 (29.5)
Collagen	31	9 (29.0)	22 (71.0)
Fat	44	32 (72.7)	12 (27.3)
Macrophages	41	20 (48.8)	21 (51.2)
IPH	42	13 (31.0)	29 (69.0)

No. = number; SD = standard deviation; IPH = intraplaque hemorrhage
Data about the histology of the plaque was not available for all patients. For the software-based data only the number of plaques are included of the available corresponding histological tissue type.
* The histology-based data was categorized in "low" and "high" presence, except for IPH, which was categorized in "absent" and "present".
† The software-based data represents the percentage of a specific tissue type compared to the whole plaque according to semi-automated software, which was used to analyze the CTA.
†† The histology-based data was measured by pathological examination and scored in subgroups of presence (low or high and in case of IPH absent or present).

Table 3.
The discriminative performance of the software by comparing the software-based proportions with the histology-based high presence of the tissue types.

Software parameter†	**Histology parameter††**	**AUC (CI 95%)**
Dense calcium	Calcifications	0.88 (0.77 - 0.98)
Fibrous	Collagen	0.69 (0.46 - 0.92)
Fibro-fatty	Fat	0.67 (0.51 - 0.84)
Necrotic core	Macrophages	0.76 (0.61 - 0.90)
Necrotic core	IPH	0.40 (0.19 - 0.60)

AUC = area under curve value; CI = confidence interval; IPH = intraplaque hemorrhage
† The software parameter defines an individual tissue type based on software used to analyze the CTA (dependent on HU values of the tissue type on CTA), measured in percentages of the whole plaque.
†† The histology parameter defines an individual tissue type based on histological examination of the culprit slice of the plaque, scored as low or high presence and in case of IPH present or absent.

Table 4.
Attenuation thresholds/values for each tissue type according to current and previous studies.

Article	Attenuation thresholds for each tissue type (in HU) (and mean attenuation per tissue type for Saba et al.)
De Weert et al.*	Lipid core: -20 to 60
	Fibrous: 60 to 140
	Calcifications: >130
Wintermark et al.*	LRNC: < 39.5
	Connective tissue: 39.5 to 72
	Hemorrhage: 72 to 177.1
	Calcification: >177.1
Varrassi et al.**	Adipose: -100 to 49
	Fibrotic: 50 to 150
	Calcifications: >150
Saba et al.***	IPH: 18.4 ± 4.8
	LRNC: 48.048 ± 19.4
	Fibrous: 93.128 ± 16.4
Current study†	Necrotic core: -30 to 75
	Fibrofatty: 76 to 130
	Fibrous: 131 to 350
	Dense calcium: >350

HU = Hounsfield unit; SD = standard deviation; LRNC = lipid rich necrotic core; IPH = intraplaque hemorrhage
* Attenuation thresholds/values based on histological tissue regions compared with HU values on CTA.
** Reasoning for attenuation thresholds unclear.
*** Mean attenuation values were described instead of attenuation thresholds. These values were based on histological tissue regions compared with HU values on CTA.
† Attenuation thresholds based on intravascular ultrasound virtual histology of coronary artery and optimized training sets.

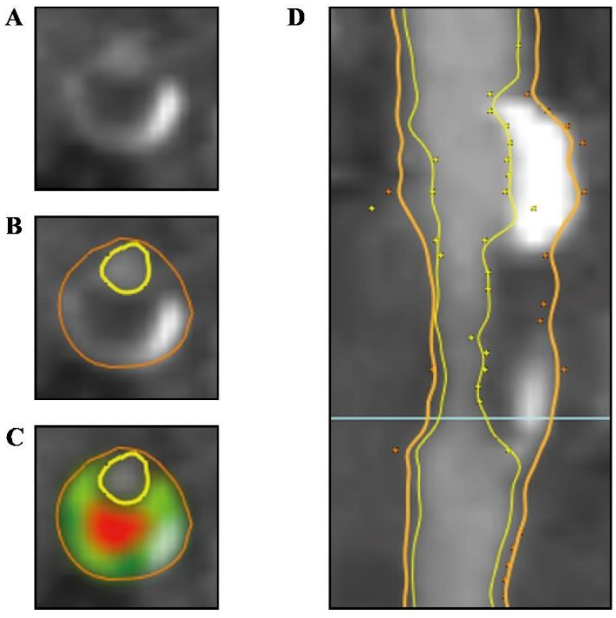

Figure 1. *Example of the QAngioCT software*
Transversal and longitudinal slice visualizing the left carotid artery, containing a narrowed lumen and an atherosclerotic plaque. (A) Transversal slice without formatting. (B) Transversal slice with additional lumen (yellow) and vessel wall (orange) contours. (C) Transversal slice with contours and color overlay defining the tissue types (red = necrotic core, light green = fibrofatty, dark green = fibrous, white = dense calcium). D, Longitudinal slice with lumen (yellow) and vessel wall (orange) contours, with a light blue line indicating the location of the transversal slice (as can be seen in A, B and C).

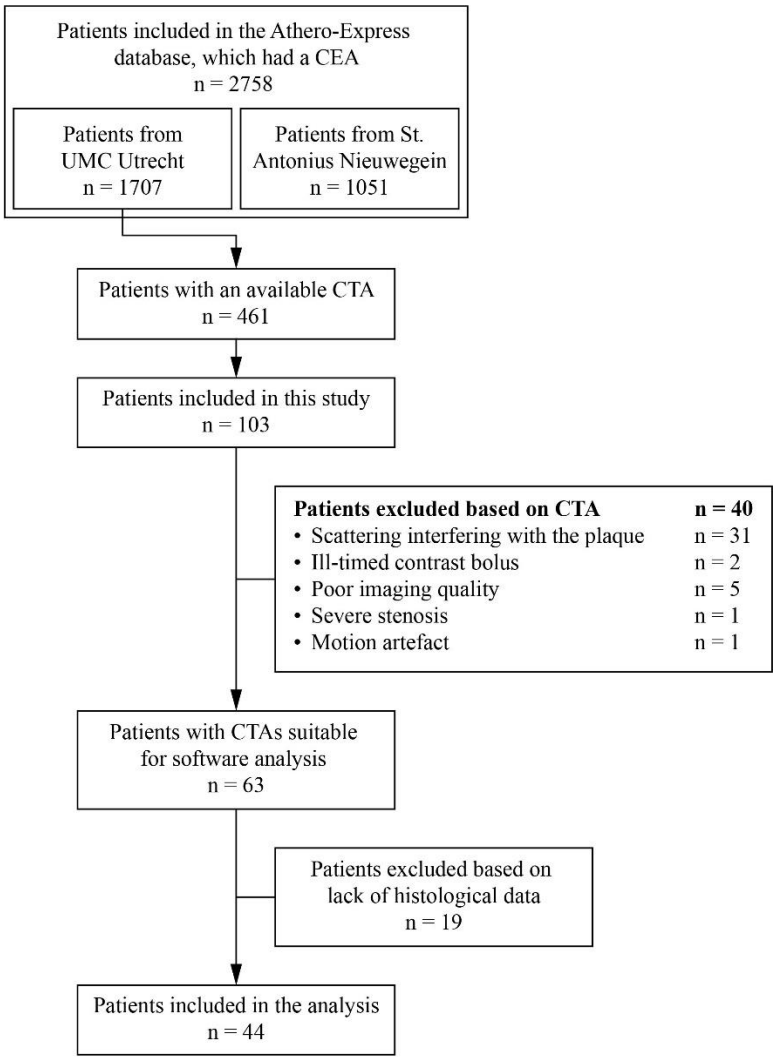

Figure 2. *Inclusion of patients based on the selection criteria*
CEA = coronary endarterectomy; UMC = University medical center; CTA = coronary tomography angiography

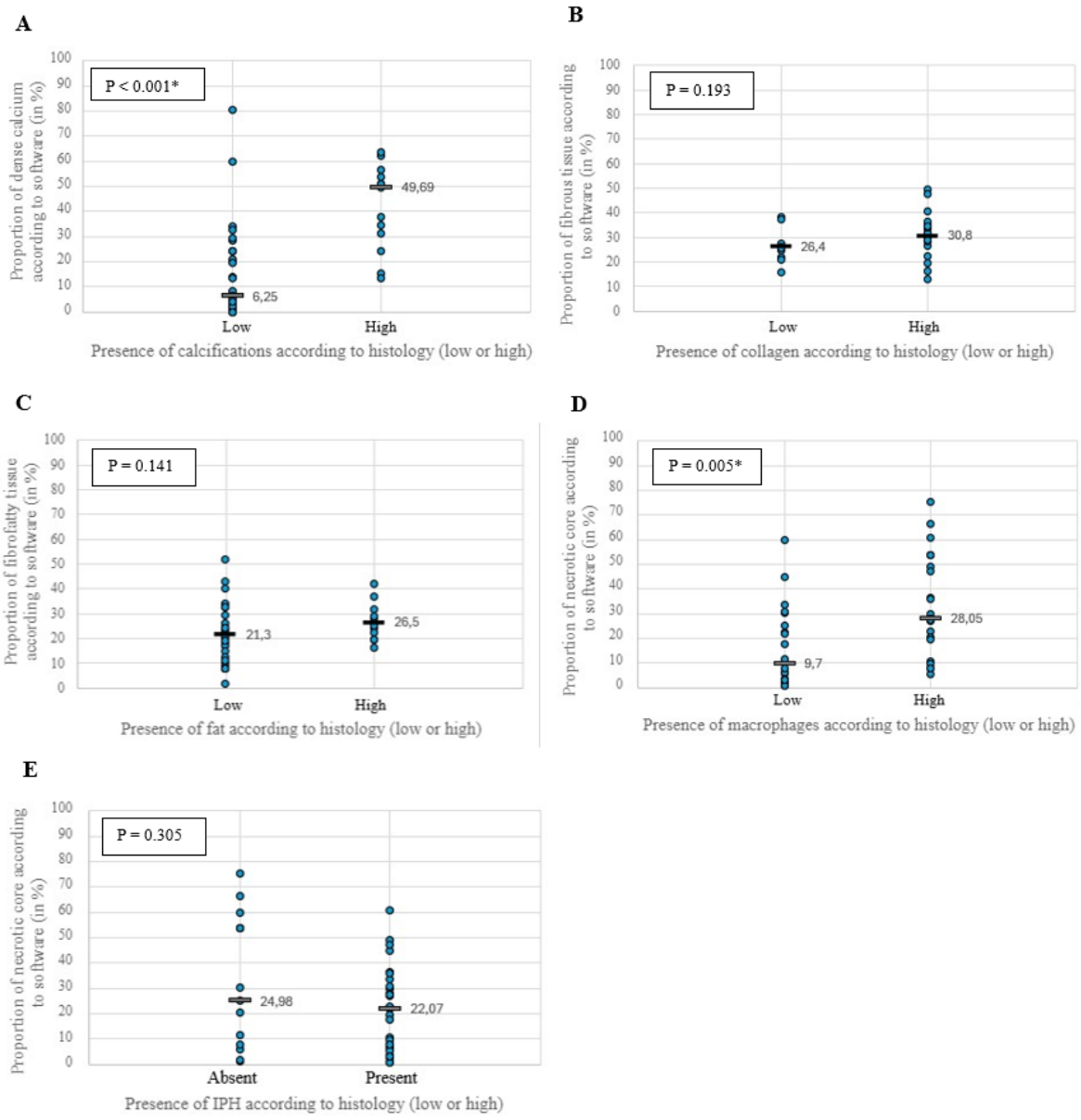

Figure 2.

Scatterplots of the distribution of the software-derived data, divided by the histological subcategories (low/absent or high/present). The p-values indicate the significance of the difference of the software-derived data between the subcategories of the histological data. For normal distribution of the continuous data (in case of B and C), the mean values are presented with black lines and the corresponding value; and the p-value was calculated with Independent Samples t-Test. For non-normal distributions of the continuous data (in case of A, D and E), the median values are presented with grey lines and the corresponding value; and the p-value was calculated with the Mann-Whitney U test. (A) Software-based dense calcium (in %) compared to the histology-based presence of calcifications (low or high). (B) Software-based fibrous tissue (in %) compared to the histology-based presence of collagen (low or high). (C) Software-based fibrofatty tissue (in %) compared to the histology-based presence of calcifications (low or high). (D) Software-based necrotic core (in %) compared to the presence of histology-based macrophages (low or high). (E) Software-based necrotic core (in %) compared to the histology-based presence of IPH (absent or present).

IPH = intraplaque hemorrhage

* P < 0.05 is significant